Metappearance: Meta-Learning for Visual Appearance Reproduction

MICHAEL FISCHER, University College London, United Kingdom TOBIAS RITSCHEL, University College London, United Kingdom

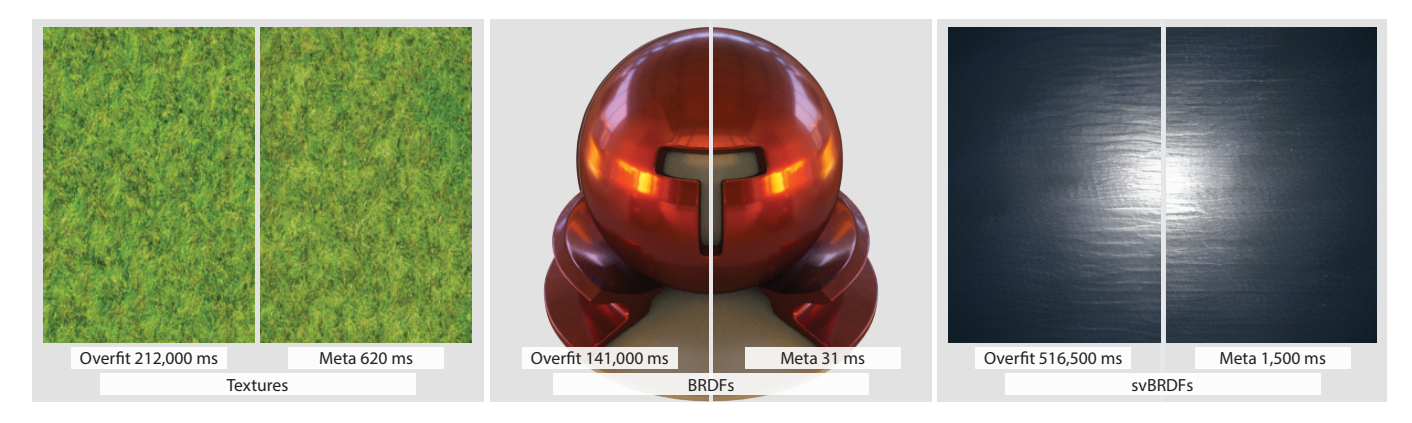


Fig. 1. We propose meta-learning for reproduction of appearance, such as textures, BRDFs or svBRDFs. Given as few as 10 optimization steps, our method (right in each subfigure) achieves quality comparable to overfit-approaches (left in each subfigure) that take orders of magnitude more training iterations.

There currently are two main approaches to reproducing visual appearance using Machine Learning (ML): The first is training models that generalize over different instances of a problem, e.g., different images from a dataset. Such models learn priors over the data corpus and use this knowledge to provide fast inference with little input, often as a one-shot operation. However, this generality comes at the cost of fidelity, as such methods often struggle to achieve the final quality required. The second approach does not train a model that generalizes across the data, but overfits to a single instance of a problem, e.g., a flash image of a material. This produces detailed and high-quality results, but requires time-consuming training and is, as mere non-linear function fitting, unable to exploit previous experience. Techniques such as fine-tuning or auto-decoders combine both approaches but are sequential and rely on per-exemplar optimization. We suggest to combine both techniques end-to-end using meta-learning: We over-fit onto a single problem instance in an inner loop, while also learning how to do so efficiently in an outer-loop that builds intuition over many optimization runs. We demonstrate this concept to be versatile and efficient, applying it to RGB textures, Bi-directional Reflectance Distribution Functions (BRDFs), or Spatially-varying BRDFs (svBRDFs).

Additional Key Words and Phrases: Visual Appearance; Deep learning; Meta-Learning; BRDFs

1 INTRODUCTION

Reproduction of visual appearance [Dorsey et al. 2010] is a key part of Computer Graphics that has achieved new levels of simplicity, speed and accuracy thanks to recent developments in Machine Learning (ML). The classic use of ML for appearance reproduction was to capture light or materials from very little input, sometimes only single images [Deschaintre et al. 2018; Georgoulis et al. 2017], without access to ground truth maps. These approaches were trained for a long time on large datasets, resulting in impressive levels of

Authors' addresses: Michael Fischer, University College London, United Kingdom, m.fischer@cs.ucl.ac.uk; Tobias Ritschel, University College London, United Kingdom, t.ritschel@ucl.ac.uk.

generalization. Unfortunately, this generality comes at the price of not matching the target precisely: we might get a great looking Bi-directional Reflectance Distribution Function (BRDF) or Spatially-varying BRDF (svBRDF) from a single image, but it is not quite the one of the input. Such approaches recognize patterns, and are predominantly based on Convolutional Neural Networks (CNNs), but this is no strict requirement.

More recently, a second line of research has evolved, where no attempt is made to generalize over a large dataset, and, instead, non-linear optimization, together with differentiable rendering is used to explain visual appearance in input images [Gatys et al. 2015; Mildenhall et al. 2020; Rainer et al. 2019]. These methods very accurately match the reference, but need many ground truth input images, take long to train and can be slow to execute. Typically, such approaches use point-operations, e.g., Multi-layered Perceptrons (MLPs), rather than CNNs.

A first step to bridge this chasm was introduced by adapting the output of a model from the general class in a second, non-differentiable step, the so-called "fine-tuning" stage [Deschaintre et al. 2020; Gao et al. 2019; Guo et al. 2020; Henzler et al. 2021]. Approaches that use fine-tuning usually run an additional number of gradient steps (in the order of magnitude 10^3) towards a specific target, which greatly improves reconstruction quality, but inflates runtime to the order of minutes, whereas the general CNN approaches are feed-forward operations in milliseconds.

In this work we make progress to further close the quality- and speed-gap between these two schools of visual appearance reproduction, and enable quality that is close to model-overfitting and fine-tuning at interactive runtimes close to those of general feed-forward networks. To this end, we dot not propose a new visual appearance method, nor do we compare methods or analyze their properties. Instead, we look into a different way to train them. This

is achieved by *meta-learning*, where we learn how to drive the optimization that over-fits the input so as to converge to the right solution in a low number of steps, typically around 10 only. Using meta-learning, we are able to speed up faithful appearance reproduction by several orders of magnitude, while keeping all desirable properties of the base approach and with similar visual quality.

This is enabled by the following contributions

- Formalizing a range of visual appearance reproduction problems in one optimization model.
- Optimizing for a fast and accurate optimizer of this model.
- Instances of that model to match texture, BRDFs, or svBRDFs orders of magnitude faster and with much fewer parameters than strong baselines at similar quality.

2 PREVIOUS WORK

2.1 Visual Appearance

We consider visual appearance reproduction, the task of generating plausible and accurate visual patterns across all positions and orientations from evidence captured for some angles and locations.

Ignoring angle and considering an exemplar's statistics, we would talk about appearance as *texture* [Efros and Leung 1999; Gatys et al. 2015; Julesz 1975]. When angle matters, we would call this Bi-directional Reflectance Distribution Function (BRDF) [Guarnera et al. 2016; Ngan et al. 2005] and when both space and orientation are considered, Spatially-varying BRDF (svBRDF) [Dana and Wang 2004]. Guarnera et al. [2016] summarize these approaches. Textures [Gatys et al. 2015; Ulyanov et al. 2016], BRDFs [Georgoulis et al. 2017] and svBRDFs [Deschaintre et al. 2018] have all been acquired and represented by means of ML, for which Tewari et al. [2020] provide a survey. We defer discussion of the specific existing solutions for all those sub-problems to Sec. 4.

2.2 Learning

More important to our problem is how the different methods are learned, i.e., optimized, given either the information of a single instance or an entire set of exemplars (Tab. 1).

Table 1. Different ways to optimize for visual appearance reproduction.

	General	Fast	Accurate	Compact
General	✓	✓	×	×
Overfit	×	×	\checkmark	\checkmark
Finetune	×	×	\checkmark	×
Meta (ours)	✓	\checkmark	\checkmark	✓

General Learning. A typical paradigm is to collect a training dataset, say, 2D images, to curate them with appearance supervision and, say, BRDF parameters, and to learn a mapping from the image to those parameters, for example through a CNN [Georgoulis et al. 2017]. Often, such methods create a latent space. While it is a strength, that this space will only contain valid exemplars, it comes at the expense of a bottleneck, reducing specific details. In simple words, a 100-dimensional latent space can make sure every latent code is a grass texture, but it cannot represent the exact location of

200 grass blades in an image. Examples of such approaches include work by Henzler et al. [2020] (texture), Georgoulis et al. [2017] (BRDF) or Deschaintre et al. [2018]; Gao et al. [2019]; Guo et al. [2020]; Kuznetsov et al. [2019] (svBRDF). These methods generalize well to new images, but do not *exactly* match the test-time input. We call these **General**.

Over-fit Optimization. A second, more classical approach is to not seek generalization, but to fit a model to one specific exemplar from the problem domain. This technique has seen a recent increase in popularity due to the emergence of coordinate-based neural representations, and often is used in conjunction with MLPs. Examples are numerous and include most works related to Neural Radiance Fields (NeRF) [Mildenhall et al. 2020] as well as others for texture [Kuznetsov et al. 2021; Sztrajman et al. 2021] and svBRDFs [Zhang et al. 2021]. We call these methods Overfit.

Fine-tuning. A combination of above approaches is sometimes used, where first a general network is trained and then, when the target instance is known, is optimized a second time [Deschaintre et al. 2020; Henzler et al. 2021]. This may, or may not, involve optimizing for latent coordinates to match the input [Tan and Mayrovouniotis 1995]. We here name these **Finetune**.

Hyper and meta-learning. Hyper and meta-learning train a network to produce weights of another network. One instance of this is hyper-networks, where a first network directly outputs the weights of a second network [Ha et al. 2016]. This has been applied to appearance [Bi et al. 2021; Maximov et al. 2019], BRDFs [Sztrajman et al. 2021] and NeRF-like representations [Sitzmann et al. 2019]. Meta-learning, instead, does not directly produce the parameters of another network, but guides the optimization that drives the inner learning. This optimization is often based on gradient descent, so the outer network produces guidance such as start values and step sizes. Sometimes, the gradient rule itself is learned [Adler and Öktem 2018]. Applications of meta-learning were proposed for geometry [Sitzmann et al. 2020], super-resolution [Hu et al. 2019] and animation [Wang et al. 2021], layered depth images [Flynn et al. 2019], as well as for NeRF [Mildenhall et al. 2020] by Bergman et al. [2021] and Tancik et al. [2021]. We would not be aware of work attempting to model visual appearance using Meta-learning, as we set out to do next.

3 OUR APPROACH

We seek to represent radiance $L_{\theta}(\mathbf{x},\omega|I)$ as a parametric function in θ , of position \mathbf{x} and direction ω , conditioned on some input I. I varies per-application and could be a single image, sparse measurements. Parameterizing L_{θ} is possible in a large number of ways, for instance through a plain, pixel-based RGB image, a CNN or an MLP, and the parametrization might involve hard-coded, rendering-like operations, or combinations thereof. We deliberately do not specify this further now and describe concrete application instances in Sec. 4.1, Sec. 4.2 and Sec. 4.3. For now, we only require L to be differentiable w.r.t. the parameters θ .

In the ML and Graphics community, there are several established ways to optimize for this notion of appearance. For one, there are **general** methods, that are trained across many *I* and generalize to new, unseen inputs (Sec. 3.1). Another approach is an **overfitting**

solution, that is trained to reproduce a single input only (Sec. 3.2). Moreover, a combination of both methods can be used, that first runs a general method and subsequently performs over-fitting through fine-tuning (Sec. 3.3). Orthogonally, we propose our meta-solution, which is an end-to-end combination of generality and fine-tuning (Sec. 3.4). To enable comparisons, we will now formalize the aforementioned approaches.

3.1 General Encoding

For generalization across all input, we typically solve

$$\arg\min_{\theta} \mathbb{E}_i \left[|L_{\theta}(\mathbf{x}_i, \omega_i | I_i) - L_i| \right], \tag{1}$$

where \mathbb{E} is the expectation across the observation I_i , the radiance L_i , the location x_i and the direction ω_i , of the *i*-th training exemplar, respectively. |-| here, and in the following, can refer to any norm, and we use the 1-norm in practice. This formulation, without loss of generality, hides the fact that this problem usually is ambiguous: One I_i can typically be explained by more than one direction ω_i or one position x_i . Over the course of training, the optimization sees many different conditions I_i and hence can build a prior about what solutions are more likely than others. This prior is then used to generalize to new conditions under new angles and positions, e.g., a new 2D photo of a sphere that can then provide reflectance for new 3D angles and 3D positions. However, the encoding of these priors that then handle variations over I must be performed under the constraint of a finite budget of parameters. In typical applications, this results in more or less subtle forms of smoothing: a generated BRDF does not quite resemble the BRDF the input specifies, some spatial details are lost in svBRDFs, etc. We will show examples of this in Sec. 4.

3.2 Over-Fitting

Differently, in over-fitting, we solve

$$\arg\min_{\theta} \mathbb{E}_i \left[|L_{\theta}(\mathbf{x}_i, \omega_i | I) - L_i| \right], \tag{2}$$

where, importantly, I is constant and does not depend on i. This task is comparatively easy, as the network only has to deal with one specific input. Consequently, results are often of higher quality than in the General setting. However, the optimization now lacks the synoptic approach that sees all instances and can use this "bigger picture" to build priors and make do with fewer information in lower time. Typically, over-fitting approaches need many iterations to train and take from minutes to hours converge, and sometimes even need further regularization, e.g., by physical constraints, to avoid over-fitting the training set.

3.3 Fine-Tuning

Both overfitting and generalization can be combined in a trivial way: First run a general method on the input, second, optimize the output so that it resembles the input even more. One instance of this is auto-decoders [Park et al. 2019; Tan and Mayrovouniotis 1995] but similar ideas were also applied to svBRDFs [Deschaintre et al. 2020; Henzler et al. 2021]. The arg min operation is commonly implemented using Gradient Descent (GD). We write $\arg \min_{A \in \mathbb{R} \to \theta}$ to denote GD starting at A to optimize θ with steps of size S (we assume different step sizes per weight, so this is a vector).

Fine-tuning usually starts from initial parameters θ_0 , that have been trained across many inputs (e.g., the converged state of a general model, cf. Sec. 3.1), and then optimizes these for a fixed target, as in over-fitting (Sec. 3.2). This means to first minimize across all inputs

$$\theta^{\star} = \arg\min_{\theta_0, S_C \to \theta} \mathbb{E}_i \left[|L_{\theta}(\mathbf{x}_i, \omega_i | I_i) - L_i| \right], \tag{3}$$

followed by optimizing for a fixed input I:

$$\arg\min_{\theta^{\star}, S_{F} \to \theta} \mathbb{E}_{i} \left[|L_{\theta}(\mathbf{x}_{i}, \omega_{i}|I) - L_{i}| \right]. \tag{4}$$

While the general projection step can be re-used across several inputs, the subsequent over-fitting optimization must be repeated for each new input. Fine-tuning usually takes in the order of minutes, i.e., it is a comparatively slow process. Moreover, there is no mechanism preventing it from diverging from the priors that informed the first step. By jointly training over both the general projection and the fine-tuning stage, we overcome these issues, as explained next.

3.4 Meta-Learning

A general model's training is agnostic to the fact that later finetuning iterations will be used to further improve the results. This drives the general projection step towards learning unnecessarily detailed representations while missing other important features and over-smoothing the space (cf. Sec. 3.1). The general step hence will try to incorporate features that fine-tuning might include anyway, and subsequently disregard other, more general elements that the fine-tuning operator might miss.

Meta-learning trades both of these aspects optimally: The model initialization can be seen as a very coarse general projection step that is later refined by a small, differentiable inner-loop optimization run. Through backpropagation of the final inner-loop gradients to the general initialization, meta-learning incorporates fine-tuning knowledge into the general model training.

We consider meta learning of both the initial solution θ_0 as well as the per-parameter step sizes S. We stack the initial parameters θ_0 and step sizes S into a meta parameter vector, denoted as $\phi = \{\theta_0, S_0\}$. Meta learning can then be formalized as

$$\arg\min_{\phi_0,S_{\mathrm{M}}\to\phi}\mathbb{E}_j\left[\arg\min_{\phi\to\theta}\mathbb{E}_i\left[\left|L_{\theta}(\mathbf{x}_i,\omega_i|I_j)-L_i\right|\right]\right]. \tag{5}$$

By encouraging network parametrizations that enable few-step convergence on new, unseen tasks, meta-learning optimizes over optimization itself. More specifically, in our scenario, the inner optimizer learns to over-fit to the appearance of one exemplar (note the dependence of I_i on j, the outer expectation, and not on i, the inner expectation). The outer optimizer then changes the inner optimizer's start parameter values, so that the next inner-loop execution will achieve improved results. This combines the quality of over-fitting with the ability to build priors of general approaches. In practice, the inner training loop takes several orders of magnitude less iterations than common over-fit training and is two or three orders of magnitudes faster than fine-tuning.

Implementation

We implement our method according to the Model-agnostic metalearning (MAML) framework proposed by Finn et al. [2017]. As the

name suggests, the meta-learner is agnostic to the inner network being used, which makes the approach flexible and well-suited for our different application scenarios.

In general, MAML works as follows: When given a task \mathcal{T} from a task distribution, we perform k steps of vanilla gradient descent on the model's parameters, this is referred to as the "inner loop". We then measure the adapted model's performance on held-out data $(\mathbf{x}_i^*, \omega_i^*)$ from \mathcal{T} and calculate the gradient of the final loss towards the parameters we started the inner loop with. We finally use this "meta-gradient", often averaged over a meta-batch of size b, to shift the initial parameters, such that in the next iteration, the inner loop will achieve better performance. Fig. 2 illustrates this idea with two very basic tasks, while we outline the algorithm structure in pseudo-code in Alg. 1. For a detailed description of the different meta-learning algorithms and implementation tools we use, please confer the supplemental, Sec. 1.

Algorithm 1 Meta-learning

```
1: procedure Innerloop(\theta)
 2:
            for i \in \{1, ..., k\} do
 3:
                  loss = |L_{\theta}(\mathbf{x}_i, \omega_i) - L_i|
                  \theta = \phi_s \cdot \operatorname{grad}(\operatorname{loss})(\theta)
 4:
 5:
           return |L_{\theta}(\mathbf{x}_{i}^{*}, \omega_{i}^{*}) - L_{i}^{*}|
 6:
 7: end procedure
 8:
     repeat
 9:
            \theta := \phi_0
           metaloss = 0
10:
            for i \in \{1, ..., b\} do
11:
                  metaloss += Innerloop(\theta)
12:
13:
            end for
            \phi_0 = 1/b \cdot S_{\mathbf{M}} \cdot \operatorname{grad}(\operatorname{metaloss})(\phi_0)
15: until converged.
```

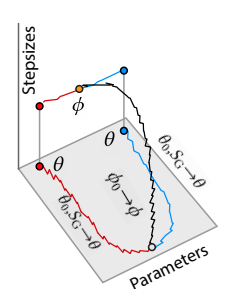


Fig. 2. Learning (blue, red) and meta-learning (black) trajectories.

4 APPLICATIONS

We demonstrate effectiveness of meta-learning for visual appearance reproduction on four increasingly complex applications: RGB textures (Sec. 4.1), BRDFs (Sec. 4.2) and svBRDFs (Sec. 4.3).

Protocol. We compare our method against the approaches listed in Sec. 3. The protocol for our evaluation is as follows: Let I denote the entire training data set, e.g., all BRDF samples in the MERL [Matusik 2003] database. For **Overfit**, we sample a single input I from I and train a network on I, and only I, until convergence. **General** denotes a network that has been trained on all elements in I and then is conditioned on the particular I we want inference for. **Finetune** applies a pre-defined number of I fine-tuning steps to the output of **General** to further improve the result for a particular I. Finally, our proposed **Meta**-learning is trained on all tasks in I, but under the constraint of being given only a fixed budget of I0 gradient descent steps, with I1 with I2 can then quickly be instantiated by updating the initial meta-model parameters I3 times.

Evaluation. We evaluate each method on unseen input from the test set, with the particular evaluation metric depending on the application. We record and report all timings on the same machine, equipped with an NVIDIA RTX 3060 Ti. Note that the speed and memory consumption of the deployed application Neural Network (NN) is unaffected by using meta-learning.

Additionally, we introduce the Error-Runtime-Ratio (ERR) $\in \mathbb{R}_0^+$, which weights the increase in runtime against the increase in performance. Given a baseline method b and a second method m which we would like to evaluate, we specifically calculate

$$ERR(\rho_{\rm m}, \rho_{\rm b}, \delta_{\rm b}, \delta_{\rm m}) = \frac{\rho_{\rm m} \cdot \rho_{\rm b}^{-1}}{\delta_{\rm b} \cdot \delta_{\rm m}^{-1}}, \tag{6}$$

where ρ and δ denote the final runtime and error, respectively. The ERR-index intuitively is the linear trade-off between runtime-increase and performance gain: A method that achieves a 10-fold reduction in error but entails a 10-fold increase in runtime scores an ERR-index of 1.0. All ERRs stated are relative to b = General.

4.1 RGB Textures

Efficient and high quality texture synthesis has many applications in content creation and visual design (for a comprehensive survey, we refer the reader to Raad et al. [2018]). We hence aim to learn a mapping that fills the infinite plane with a pattern whose statistics are close to those of a given reference image. We do so by directly optimizing for the Mean Absolute Error (MAE) between the Gram Matrices of VGG activations [Gatys et al. 2015].

Previous work. Famously, Gatys et al. [2015] optimized for a finite image in pixel space such that its VGG activation statistics match the exemplar. Later, Ulyanov et al. [2016] trained a single CNN to perform this task feed-forward. Huang and Belongie [2017] have shown how control over (instance) normalization can produce new textures. Henzler et al. [2020] show how to do do this conditioned on an input image. These methods are exemplary for the spectrum we challenge: either they take long to learn and fit the input, or they are fast and do not fit the input exactly.

Architecture. We use a U-Net [Ronneberger et al. 2015] CNN with residual skip connections and AdaIN blocks [Huang and Belongie 2017], as proposed in [Henzler et al. 2021]. For the exact network and training setup, please confer the supplemental, Sec. 2.1.

Results. We summarize quantitative results in Tab. 2. We consistently show lower compute time than Finetune and Overfit at similar quality and much lower parameter count (we use only 11.3% of the weights of General or Finetune). The ERR measure for combining speed and quality is better by one order of magnitude or more for Meta (ours).

Fig. 3 shows qualitative results that further confirm these quantitative findings. **General** often projects the unseen textures into the latent space only approximately, which results in subtle but noticeable differences in features, color and scale. **Finetune** and **Overfit** both almost perfectly replicate the original, as both methods conduct a complete optimization run on the current sample. Our **Meta**-method faithfully replicates all textures with only minor differences in style.

Fig. 4 visualizes the convergence behaviour for the different methods. It is evident that the fast one-step projection of General entails

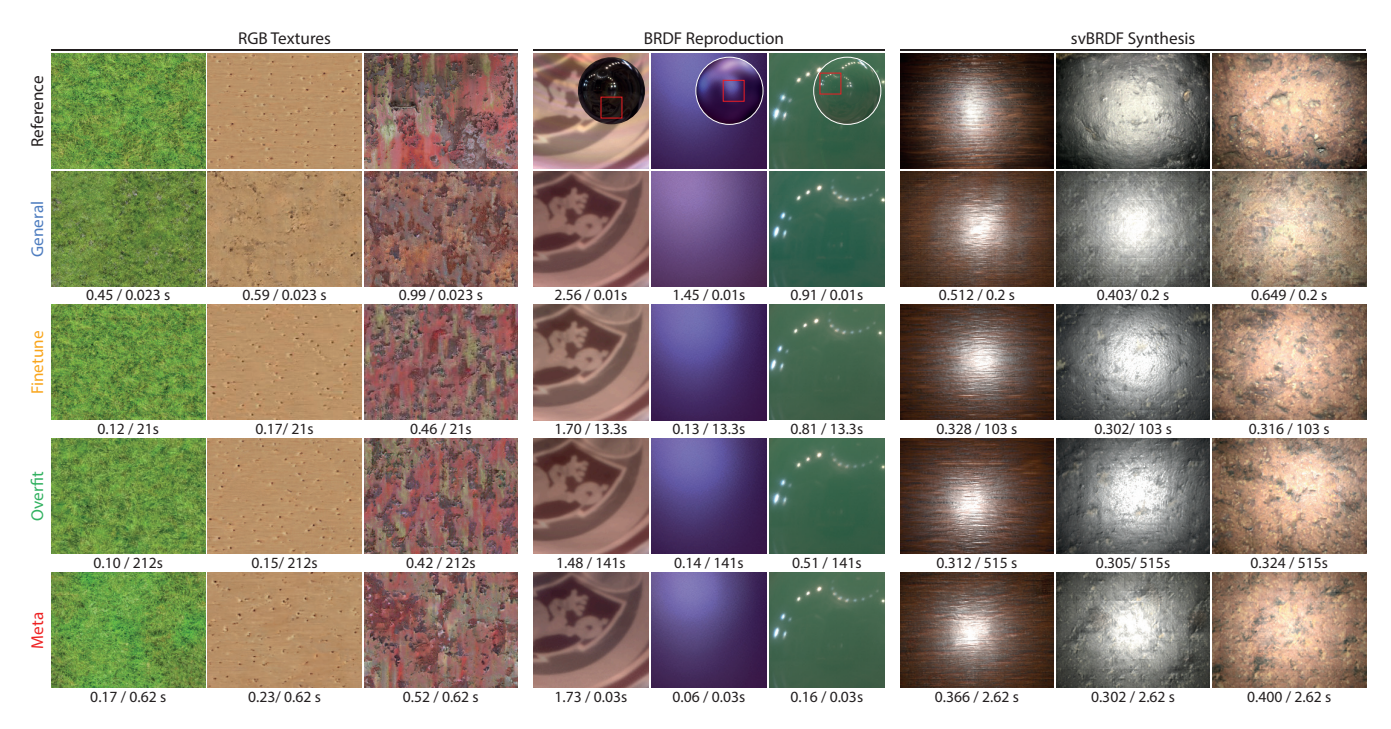


Fig. 3. We show results across the test-set of each respective application. For the BRDF results, we show an inset of a sphere rendered under environment illumination. We report error and runtime for each image (VGG Gram matrix L1 for texture and svBRDF, MAE for BRDF, lower is better for all metrics.). In terms of error, our method consistently outperforms General, and performs on par with Finetune and Overfit. In terms of speed, ours is much closer to General than optimization-based methods. For the full range of our results, please see the supplemental materials.

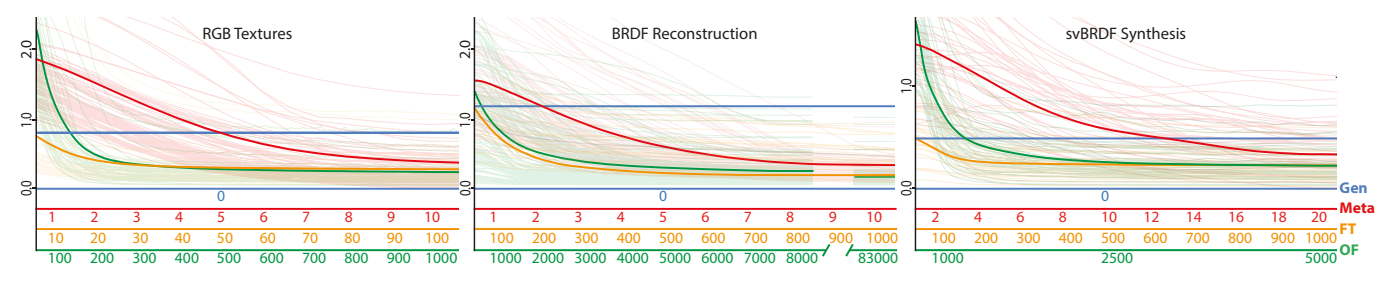


Fig. 4. Error (vertical) of the different methods across our three sample applications (horizontal). We report VGG Style Error for textures and svBRDFs and logarithmic MAE in reconstruction space for BRDF encoding. Each method is a color and every line is a problem instance, e.g., a texture that is to be fit. Thick lines are means for each method, thin lines are the individual fits. Note that the horizontal axis differs drastically for all methods.

Table 2. Quantitative results across all applications, lower is better, except for SSIM, where higher is better. We report MAE and SSIM in image space, when rendering the resulting neural BRDFs on a sphere under environment illumination. For fairness, we include our learned per-parameter learning rate in the parameter comparison. Inference time denotes the time it takes to produce an output, conditioned on the input, for a new, unseen image for the first time.

	RGB Texturing				BRDF Reconstruction				svBRDF Synthesis				
	VGG Error	Params	Time	ERR	MAE	SSIM	Params	Time	ERR	VGG Error	Params	Time	ERR
General	0.79	48.58 M	0.02	_	1.89	0.981	4.3 M	0.005	_	0.43	48.58 M	0.2	_
Overfit	0.24	$2.74\mathrm{M}$	212.00	3220.3	0.63	0.994	675	141.000	9400.0	0.22	$2.74\mathrm{M}$	516.5	1321.2
Finetune	0.27	48.58 M	21.20	362.3	0.65	0.993	4.3 M	9.974	686.0	0.25	48.58 M	103.1	299.7
Meta (ours)	0.39	5.47 M	0.62	15.3	0.72	0.990	1.350	0.031	2.4	0.31	5.48 M	1.5	5.4

a significant decrease in performance compared to all other methods. Finetune, starting from the output of General, requires around 100 additional steps to converge to similar high-quality results as Overfit after 1000 steps. Meta bridges this chasm between runtime and quality by providing results that are close to the outputs of Finetune and Overfit in only 10 gradient steps.

Compression. Our Meta-method can further be interpreted as a compression scheme. Consider a rendering or 3D-modeling application, e.g., Blender, that loads a pre-trained model's weights to create new, diverse textures for surfaces. With methods Overfit and Finetune, such an application would have to store an entire set of weights per texture to be generated (note that, in such a scenario, storing the fine-tuned decoder of method Finetune is sufficient), and then is restricted to synthesizing the pre-learned texture exemplars. One could alternatively store the heavy-weight general model, but then would either have to forego accurate high-quality synthesis or fine-tune the result, which is unsatisfying and time-consuming, respectively. With our proposed Meta-method, it is sufficient to store two sets of weights only (the model's weights, and the perparameter learning rate) to achieve high-quality, diverse texture synthesis in interactive runtime, i.e., in less than a second.

Let w denote the number of disk space required to store the decoder's weights in methods **Overfit** and **Finetune**. The total amount of storage required for the efficient and exact synthesis of m textures then equals wm. Our **Meta**-method achieves similar-quality results with *constant* storage requirement 2w, and is not limited to pre-trained or fine-tuned texture exemplars but instead can quickly infer new, unseen exemplars with high fidelity. The compression factor our method achieves hence is $2m^{-1}$, which, in the case of this texture application with 500 exemplars, equals 1:250.

4.2 BRDFs

While the RGB textures varied in space, but not in angle, we now look into visual appearance varying with angle, but not over space, the classic BRDF representation task. For our experiments, we use the MERL [Matusik 2003] BRDF database.

Previous Work. Much work was devoted to create, efficiently compress, interpolate and re-sample (spaces of) BRDFs; for a general survey we refer to Guarnera et al. [2016]. Many applications revolve around representing a full BRDF in high quality from a small set of measurements. When these are taken in a suitable pattern [Nielsen et al. 2015], a linear basis found through Principal Component Analysis (PCA) can be used as an encoding. Recently, Rainer et al. [2019] showed that NN-based encoding of radiance data is a viable alternative to traditional, PCA-based methods. Moreover, [Hu et al. 2020] and [Rainer et al. 2020] encode multiple BRDFs and Bidirectional Texture Functions (BTFs) in a single network, respectively. Finally, Sztrajman et al. [2021] show that a simple two-layer MLP can learn the mapping between angular measurements and RGB reflectance and is able to faithfully reproduce BRDFs.

Architecture. Our method follows Sztrajman et al. [2021] and Hu et al. [2020]. Details on the architecture and the different algorithm setups are found in the supplemental materials, Sec. 2.2.

Results. Our Meta-method achieves high fidelity reproduction results across all BRDFs in the MERL-database, as quantified in

Tab. 2. When rendered under Paul Debevec's St. Peter's Basilica illumination, Meta achieves Structural Similarity (SSIM) values of ≥ 0.95 on 99% of all materials. For a visual comparison of the reproduction results of the different approaches, cf. Fig. 3: Our method picks up fine nuances in the BRDF correctly, and we consistently show large improvements over General. In some cases, Meta even outperform methods Finetune and Overfit, which both have a gradient descent budget several orders of magnitudes larger than our method. This is also reflected in Fig. 4, where we plot the convergence behaviour of the different approaches over the duration of the model-training: Overfit evidently achieves the lowest training error, closely followed by Finetune. Our Meta-method manages to achieve similar performance in only k=10 steps. Moreover, our method provides the highest performance gain when weighted against the increase in runtime and scores an ERR of only 2.1.

Meta will converge to a loss difference of less than 1 % relative to Overfit in only 65 additional training steps (5 seconds). Related, General will not improve from further training and has been trained to saturation already.

Sample efficiency. Note that, as a we are using a small number of steps with a small batch size, our method sees much fewer data than all competitors: during inference, we sample a batch with 512 samples for each inner-loop step, which leads to a total of 5120 samples (< 0.5%) processed by our method, while the competitors have access to all 1.46×10^6 measurements of the MERL BRDF.

Compression. In this scenario, our Meta-method achieves compression in two separate ways. First, the compression argument from Sec. 4.1 can be repeated: While it requires wm space to store a model of size w for each example in a dataset of size m, our method only requires constant storage 2w for the entire dataset. The compression factor we achieve for storage hence is 1:50, as there are 100 BRDFs in the MERL database. Moreover, a NBRDF has a significantly smaller memory footprint than regular BRDFs (28 kB vs. 34.2 MB in the case of our Meta-NBRDF) so we additionally compress the original BRDF with a factor of approx. 1: 2000. Second, compression here also applies to bandwidth at inference time, i.e., the amount of data needed for a model to correctly replicate a MERL BRDF. While General, Finetune and Overfit all require the entire $540 \times 90 \times 90$ MERL measurements, our method can infer a correct MERL representation with only 5120 samples. The compression factor we achieve for bandwidth hence is $5120:1.45\times10^6\approx1:285.$

4.3 Stationary svBRDFs

The next-higher level of complexity are spatially varying BRDFs that combine spatial and angular variation of reflectance. We aim to solve the problem of estimating stationary svBRDFs from flash images, pioneered by Aittala et al. [2016].

Previous Work. The survey by Guarnera et al. [2016] also covers spatial variation. Classically, svBRDF were acquired by optimization [Lensch et al. 2003] involving appropriate priors [Dror et al. 2001; Lombardi and Nishino 2012; Nam et al. 2018], optimization in a neural representation [Aittala et al. 2016; Liu et al. 2017] and finally methods that solve the task using a feed-forward network [Henzler et al. 2021]. Optimization is either performed in the pixel basis [Aittala et al. 2016], or in a latent space [Gao et al. 2019; Guo et al.

2020; Henzler et al. 2021]. For the latter, a user has to control at which learning iteration to change form latent space to pixel-space so as to have a chance of precisely matching the target. The theme recurs: optimization is slow but matches the target well, while feedforward NNs are fast, but often do not reproduce the target.

Architecture. We implement a noise-conditioned encoder-decoder approach to solve this problem, as demonstrated in [Henzler et al. 2021]. For details on network architecture and the training routines, please cf. the supplemental, Sec. 2.3.

Results. We detail quantitative results in Tab. 2 and show qualitative results in Fig. 3. This application again confirms our the previous findings: General is fast, but fails to match the input accurately. This becomes evident in Fig. 3, where General broadly matches the target, but is missing fine details and has slightly tinted colors is slightly off (left row). In the right and middle row, the shading parameters are not correctly mapped, resulting in a washed-out highlight and an over-bright flash, respectively. Both Finetune and Overfit match the target well and pick up subtle details such as the wood grain and shading cues correctly, but take long to converge (cf. Fig. 4). Our proposed Meta-method achieves similar visual quality in a fraction of their runtime and manages to produce correct svBRDF maps in under 3 seconds. Once again, meta-learning produces the lowest ERR score and hence is the best trade-off between speed and accuracy.

Compression. We repeat the compression argument from Sec. 4.1: given a model with size w and a dataset with m tasks, methods General, Finetune and Overfit require wm storage to reproduce the dataset and then deliver unsatisfactory quality (General) or cannot infer new, unseen svBRDFs, while our Meta-method achieves results of high fidelity and requires constant storage 2w only. In the case of this svBRDF application with 346 different material classes, this equals a compression ratio of 1:173.

ANALYSIS

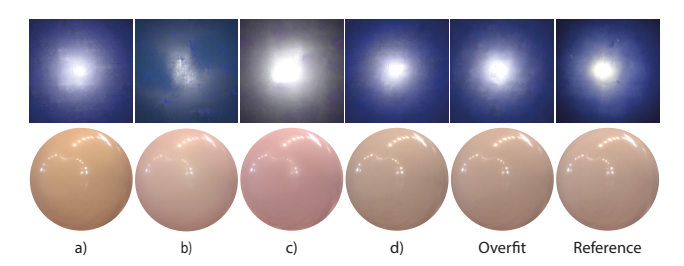


Fig. 5. We compare the influence of a learned learning rate (column b) and initialization (column c). Cf. the main text for details

In Fig. 5, we decompose the contribution of our meta-learned parameters ϕ ; initialization and step-size. In column a), we display the output of General. In column b), we take this as starting point and use our learned per-parameter learning rate to perform 20 "smart" gradient steps towards the reference. Evidently, this leads to inferior results, as the general model has not been trained to account for gradient steps of different magnitude. In column c), we use our metalearned initialization to perform k = 20 steps of Adam optimization (learning rate multiplied by 10 for faster convergence) towards the

reference. This again leads to poor results, as our learned initialization normally is adapted through large, non-uniform gradient steps. During meta-training, the initialization was hence moved to a region of the objective space that is approximately equally wellsuited for all tasks, but not necessarily easy to navigate with uniform gradient steps. Column d) shows the output of our Meta-method, where learned initialization and stepsize are used in combination. Evidently, this outperforms all alternative configurations.

This decay in reproduction quality shows that meta-learning really combines the best of both worlds: By optimizing for optimization directly, the outer optimizer can discover gradient paths that lead to local minima by not only moving the network weights (as would General), but also the step-size with which these weights are updated for a certain number of iterations (as in Finetune).

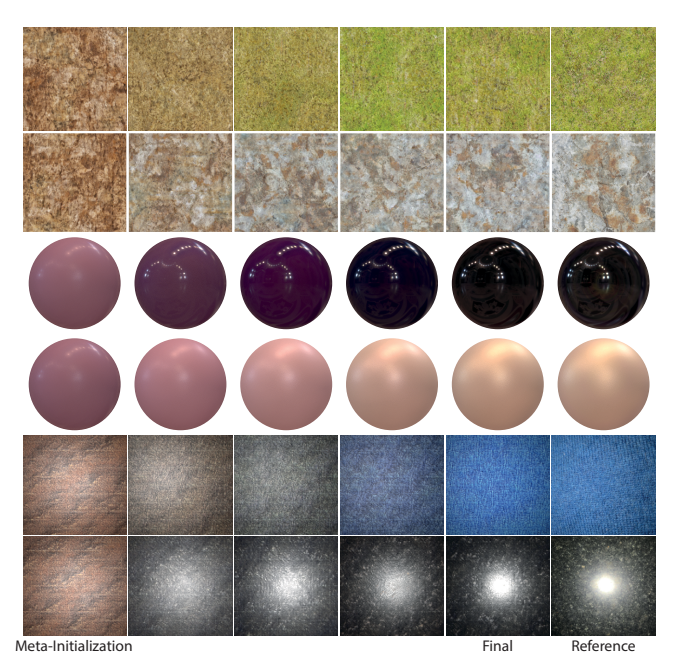


Fig. 6. Convergence from the meta-init (left) to different targets (right).

In Fig. 6, we show the convergence of our meta-learned initialization (leftmost column) towards different targets. All intermediate outputs show realistic appearance, and even the meta-initialization could pass as a problem instance (e.g., a texture) on its own. Throughout optimization, our method does not introduce unwanted artifacts, even for the ambiguous single-image svBRDF estimation task.

All experiments report the inference cost, the time between receiving a texture/BRDF/svBRDF input and outputting the answer, i.e., it does not state the meta-training time cost, which is roughly twice the one of common training.

CONCLUSION

We have used meta-learning for efficient and accurate appearancereproduction on three applications of increasing complexity. By meta-learning across different problem instances and incorporating

overfitting into the optimization process, our meta-method performed well above the general architecture throughout all applications, and often on-par with methods Finetune and Overfit.

Directions for future research could include meta-learning the objective function itself and online meta-learning for appearance reproduction. This would enable even more accurate reproduction of appearance.

ACKNOWLEDGMENTS

This work was supported by Meta Reality Labs, Grant Nr. 5034015.

REFERENCES

- Jonas Adler and Ozan Öktem. 2018. Learned primal-dual reconstruction. IEEE transactions on medical imaging 37, 6 (2018).
- Miika Aittala, Timo Aila, and Jaakko Lehtinen. 2016. Reflectance modeling by neural texture synthesis. ACM Trans. Graph. (Proc. SIGGRAPH) 35, 4 (2016).
- Alexander William Bergman, Petr Kellnhofer, and Gordon Wetzstein. 2021. Fast training of neural lumigraph representations using meta learning. In NIPS.
- Sai Bi, Stephen Lombardi, Shunsuke Saito, Tomas Simon, Shih-En Wei, Kevyn Mcphail, Ravi Ramamoorthi, Yaser Sheikh, and Jason Saragih. 2021. Deep relightable appearance models for animatable faces. ACM Transactions on Graphics (TOG) 40, 4 (2021),
- Robert L Cook and Kenneth E. Torrance. 1982. A reflectance model for computer graphics. ACM Trans. Graph. 1, 1 (1982).
- Kristin J Dana and Jing Wang. 2004. Device for convenient measurement of spatially varying bidirectional reflectance. JOSA A 21, 1 (2004).
- Tristan Deleu, Tobias Würfl, Mandana Samiei, Joseph Paul Cohen, and Yoshua Bengio. 2019. Torchmeta: A Meta-Learning library for PyTorch. arXiv:1909.06576
- Valentin Deschaintre, Miika Aittala, Fredo Durand, George Drettakis, and Adrien Bousseau, 2018. Single-image sybrdf capture with a rendering-aware deep network. ACM Trans. Graph. (Proc. SIGGRAPH) 37, 4 (2018).
- Valentin Deschaintre, George Drettakis, and Adrien Bousseau. 2020. Guided Fine-Tuning for Large-Scale Material Transfer. In Comp. Graph. Forum, Vol. 39.
- Julie Dorsey, Holly Rushmeier, and François Sillion. 2010. Digital modeling of material appearance. Elsevier.
- Ron O Dror, Edward H Adelson, and Alan S Willsky. 2001. Recognition of surface reflectance properties from a single image under unknown real-world illumination. CVPR (2001).
- Alexei A Efros and Thomas K Leung. 1999. Texture synthesis by non-parametric sampling. In ICCV.
- Chelsea Finn, Pieter Abbeel, and Sergey Levine. 2017. Model-agnostic meta-learning for fast adaptation of deep networks. In ICML.
- John Flynn, Michael Broxton, Paul Debevec, Matthew DuVall, Graham Fyffe, Ryan Overbeck, Noah Snavely, and Richard Tucker. 2019. Deepview: View synthesis with learned gradient descent. In CVPR.
- Duan Gao, Xiao Li, Yue Dong, Pieter Peers, Kun Xu, and Xin Tong. 2019. Deep inverse rendering for high-resolution SVBRDF estimation from an arbitrary number of images. ACM Trans. Graph. 38, 4 (2019), 134-1.
- Leon A Gatys, Alexander S Ecker, and Matthias Bethge. 2015. A neural algorithm of artistic style. arXiv:1508.06576 (2015).
- Stamatios Georgoulis, Konstantinos Rematas, Tobias Ritschel, Efstratios Gavves, Mario Fritz, Luc Van Gool, and Tinne Tuytelaars. 2017. Reflectance and natural illumination from single-material specular objects using deep learning. IEEE PAMI 40, 8 (2017).
- Ian J Goodfellow, Jonathon Shlens, and Christian Szegedy. 2014. Explaining and harnessing adversarial examples. arXiv preprint arXiv:1412.6572 (2014).
- Darya Guarnera, Giuseppe Claudio Guarnera, Abhijeet Ghosh, Cornelia Denk, and Mashhuda Glencross. 2016. BRDF representation and acquisition. 35, 2 (2016).
- Yu Guo, Cameron Smith, Miloš Hašan, Kalyan Sunkavalli, and Shuang Zhao. 2020. MaterialGAN: reflectance capture using a generative svBRDF model. arXiv:2010.00114
- David Ha, Andrew Dai, and Quoc V Le. 2016. Hypernetworks. arXiv:1609.09106 (2016). Kaiming He, Xiangyu Zhang, Shaoqing Ren, and Jian Sun. 2016. Deep residual learning for image recognition. In CVPR.
- Philipp Henzler, Valentin Deschaintre, Niloy J Mitra, and Tobias Ritschel. 2021. Generative Modelling of BRDF Textures from Flash Images. ACM Trans Graph (Proc SIGGRAPH Asia) 40, 5 (2021).
- Philipp Henzler, Niloy J Mitra, and Tobias Ritschel. 2020. Learning a neural 3d texture space from 2d exemplars. In CVPR.
- Bingyang Hu, Jie Guo, Yanjun Chen, Mengtian Li, and Yanwen Guo. 2020. DeepBRDF: A Deep Representation for Manipulating Measured BRDF. In Comp. Graph. Forum, Vol. 39.

- Xuecai Hu, Haoyuan Mu, Xiangyu Zhang, Zilei Wang, Tieniu Tan, and Jian Sun. 2019. Meta-SR: A magnification-arbitrary network for super-resolution. In CVPR
- Xun Huang and Serge Belongie. 2017. Arbitrary style transfer in real-time with adaptive instance normalization. In ICCV.
- Wenzel Jakob. 2010. Mitsuba renderer. http://www.mitsuba-renderer.org.
- Bela Julesz. 1975. Experiments in the visual perception of texture. Scientific American 232, 4 (1975).
- Alexandr Kuznetsov, Milos Hasan, Zexiang Xu, Ling-Qi Yan, Bruce Walter, Nima Khademi Kalantari, Steve Marschner, and Ravi Ramamoorthi. 2019. Learning generative models for rendering specular microgeometry. ACM Trans. Graph. 38, 6
- Alexandr Kuznetsov, Krishna Mullia, Zexiang Xu, Miloš Hašan, and Ravi Ramamoorthi. 2021. NeuMIP: multi-resolution neural materials. ACM Trans. Graph. (Proc. SIGGRAPH) 40, 4 (2021).
- Hendrik PA Lensch, Jan Kautz, Michael Goesele, Wolfgang Heidrich, and Hans-Peter Seidel. 2003. Image-based reconstruction of spatial appearance and geometric detail. ACM Trans. Graph. 22, 2 (2003).
- Zhenguo Li, Fengwei Zhou, Fei Chen, and Hang Li. 2017. Meta-sgd: Learning to learn quickly for few-shot learning. arXiv:1707.09835 (2017).
- Guilin Liu, Duygu Ceylan, Ersin Yumer, Jimei Yang, and Jyh-Ming Lien. 2017. Material editing using a physically based rendering network. In CVPR.
- Stephen Lombardi and Ko Nishino. 2012. Reflectance and natural illumination from a single image. In ECCV, Springer,
- Wojciech Matusik. 2003. A data-driven reflectance model. Ph.D. Dissertation. Massachusetts Institute of Technology. Maxim Maximov, Laura Leal-Taixé, Mario Fritz, and Tobias Ritschel. 2019. Deep
- appearance maps. In ICCV.
- Ben Mildenhall, Pratul P Srinivasan, Matthew Tancik, Jonathan T Barron, Ravi Ramamoorthi, and Ren Ng. 2020. Nerf: Representing scenes as neural radiance fields for view synthesis. In ECCV.
- Giljoo Nam, Joo Ho Lee, Diego Gutierrez, and Min H Kim. 2018. Practical svbrdf acquisition of 3d objects with unstructured flash photography. ACM Trans. Graph. (TOG) 37, 6 (2018).
- Addy Ngan, Frédo Durand, and Wojciech Matusik, 2005. Experimental Analysis of BRDF Models. Rendering Techniques (2005).
- Alex Nichol, Joshua Achiam, and John Schulman. 2018. On first-order meta-learning algorithms. arXiv:1803.02999 (2018).
- Jannik Boll Nielsen, Henrik Wann Jensen, and Ravi Ramamoorthi. 2015. On optimal, minimal BRDF sampling for reflectance acquisition. ACM Trans. Graph. (Proc. SIGGRAPH Asia) 34, 6 (2015)
- Jeong Joon Park, Peter Florence, Julian Straub, Richard Newcombe, and Steven Lovegrove. 2019. DeepSDF: Learning continuous signed distance functions for shape representation. In CVPR.
- Adam Paszke, Sam Gross, Francisco Massa, Adam Lerer, James Bradbury, Gregory Chanan, Trevor Killeen, Zeming Lin, Natalia Gimelshein, Luca Antiga, Alban Desmaison, Andreas Kopf, Edward Yang, Zachary DeVito, Martin Raison, Alykhan Tejani, Sasank Chilamkurthy, Benoit Steiner, Lu Fang, Junjie Bai, and Soumith Chintala. 2019. PyTorch: An Imperative Style, High-Performance Deep Learning Library. In NIPS.
- Lara Raad, Axel Davy, Agnès Desolneux, and Jean-Michel Morel. 2018. A survey of exemplar-based texture synthesis. Annals of Mathematical Sciences and Applications 3, 1 (2018).
- Gilles Rainer, Abhijeet Ghosh, Wenzel Jakob, and Tim Weyrich. 2020. Unified neural encoding of BTFs. In Comp. Graph. Forum, Vol. 39.
- Gilles Rainer, Wenzel Jakob, Abhijeet Ghosh, and Tim Weyrich. 2019. Neural BTF compression and interpolation. In Comp. Graph. Forum, Vol. 38.
- Olaf Ronneberger, Philipp Fischer, and Thomas Brox. 2015. U-net: Convolutional networks for biomedical image segmentation. In MICCAL
- Szymon M Rusinkiewicz. 1998. A new change of variables for efficient BRDF representation. In EGWR.
- Vincent Sitzmann, Eric R Chan, Richard Tucker, Noah Snavely, and Gordon Wetzstein. 2020. MetaSDF: Meta-learning signed distance functions. arXiv:2006.09662 (2020).
- Vincent Sitzmann, Michael Zollhöfer, and Gordon Wetzstein. 2019. Scene representation networks: Continuous 3d-structure-aware neural scene representations. arXiv:1906.01618 (2019)
- Alejandro Sztrajman, Gilles Rainer, Tobias Ritschel, and Tim Weyrich. 2021. Neural BRDF Representation and Importance Sampling. In Comp. Graph. Forum, Vol. 40.
- Shufeng Tan and Michael L Mayrovouniotis. 1995. Reducing data dimensionality through optimizing neural network inputs. AIChE Journal 41, 6 (1995)
- Matthew Tancik, Ben Mildenhall, Terrance Wang, Divi Schmidt, Pratul P Srinivasan, Jonathan T Barron, and Ren Ng. 2021. Learned initializations for optimizing coordinate-based neural representations. In CVPR.
- Ayush Tewari, Ohad Fried, Justus Thies, Vincent Sitzmann, Stephen Lombardi, Kalyan Sunkavalli, Ricardo Martin-Brualla, Tomas Simon, Jason Saragih, Matthias Nießner, et al. 2020. State of the art on neural rendering. In Comp. Graph. Forum, Vol. 39.

- $\label{lem:point} Dmitry Ulyanov, Vadim Lebedev, Andrea Vedaldi, and Victor S Lempitsky. 2016. Texture networks: Feed-forward synthesis of textures and stylized images.. In \emph{ICML}.$
- Shaofei Wang, Marko Mihajlovic, Qianli Ma, Andreas Geiger, and Siyu Tang. 2021. MetaAvatar: Learning Animatable Clothed Human Models from Few Depth Images. arXiv:2106.11944 (2021).
- Xiuming Zhang, Pratul P Srinivasan, Boyang Deng, Paul Debevec, William T Freeman, and Jonathan T Barron. 2021. NeRFactor: Neural Factorization of Shape and Reflectance Under an Unknown Illumination. arXiv:2106.01970 (2021).

A META-LEARNING

As denoted in the main text, we use different meta-learning algorithms for the respective applications. This originates from the fact that, in order to compute the meta-gradients, one must backpropagate through backpropagation itself, which is a very computeintensive process, as higher-order gradients (more specifically, the Hessian-vector product) must be calculated throughout the computation graph. To alleviate the computational burden this imposes, several MAML-variants that use first-order gradient approximations have been proposed. One of those algorithms that finds use in this work is First-Order MAML (FOMAML) [Finn et al. 2017], which approximates higher-order gradients by replacing the Hessian with the identity-matrix and hence updates the meta-objective with the most recent inner-loop gradient, with significant savings on GPU memory and compute time. In practice, this means that, while MAML directly optimizes over the single gradient steps that are taken to reach a solution, FOMAML approximates this highdimensional gradient trajectory with the local gradient of its last vertex. FOMAML has been shown to produce results close to MAML on certain applications [Finn et al. 2017; Nichol et al. 2018], which is commonly attributed to the fact that ReLU networks behave almost linear in high-dimensional spaces [Goodfellow et al. 2014], which in turn implies that their derivatives do not carry much second-order gradient information and can be ommitted without severe performance penalties. We also experimented with Reptile [Nichol et al. 2018], but observed no performance improvements. For the exact algorithm setup, please confer the following application subsections in this supplemental.

Note that using MAML is only compute- and memory-intensive during the meta-training phase: for inference, we run a mere gradient descent on the model parameters, and no additional overhead is incurred. We observed performance increase across all tasks and applications when also meta-learning the inner-loop learning rate, as proposed by Li et al. [2017]. We implement our meta-networks and competitors in PyTorch [Paszke et al. 2019] and Torchmeta [Deleu et al. 2019].

B NETWORKS AND IMPLEMENTATION DETAILS

We summarize the exact hyperparameters and algorithm setups in Tab. A1. The following sections shortly elaborate on the choice of models and approaches we use for the respective applications.

B.1 RGB Textures

To solve the task of texture synthesis, we use a U-Net [Ronneberger et al. 2015] CNN with residual skip connections and AdaIN blocks [Huang and Belongie 2017]. As in [Gatys et al. 2015], we optimize for the mean absolute error of VGG matrices between the reference exemplar and the network's output. The architecture is similar to Henzler et al. [2021] and we refer to their publication for the exact network details. We use this architecture as our method <code>Overfit</code> and empirically determined that 1000 training iterations are sufficient to replicate most textures faithfully.

Method General preprends a ResNet-based encoder (ResNet-50, [He et al. 2016]) to the aforementioned U-Net in order to project the input image into a latent space, from where the previously

mentioned U-Net decoder, conditioned on the latent code $z \in \mathbb{R}^{64}$, reconstructs the exemplar's features.

Finetuning has been applied in recent publications to steer the output of a general model towards more accurate representations [Deschaintre et al. 2020; Guo et al. 2020; Henzler et al. 2021].

Note that, for fine-tuning, we increase the learning rate by a factor of 10, as in Henzler et al. [2021], to accelerate convergence, which makes Finetune a strong baseline.

For our Meta-method, we found a higher number of inner-loop steps to outperform the gains from second-order gradients, and hence use FOMAML with k=10 inner-loop steps.

To show that we compare our meta-method against the best-configured competitors, we ran several experiments to empirically determine the best-suited optimizer and learning-rate setting. The results of these experiments are depicted in Tab. 2, while we show results on unseen test-data in Fig. B1. For all test-results, please see the electronic supplemental.

B.2 BRDF Reconstruction

To tackle the task of BRDF reconstruction, we use a simple two-layer MLP with 21 neurons per hidden layer, as described by Sztrajman et al. [2021], as method <code>Overfit</code>. The network receives randomly sample batches of light- and view-direction in Rusinkiewicz [1998] parametrization and then outputs the logarithmic RGB reflectance for these query directions. We train our competitor <code>Overfit</code> as described in [Sztrajman et al. 2021] (also cf. Tab. A1) with one network per MERL-material.

For General, we take inspiration from [Hu et al. 2020] and create a latent space of BRDFs by training a encoder CNN (for the exact details of the architecture we refer to their publication) that consumes the entire BRDF measurement of $540\times90\times90$ RGB triplets at once. To enable an fair comparison between our methods, we use the two-layer MLP of Sztrajman et al. [2021] as a decoder. For Finetune, we fine-tune the output of General for 1000 iterations, which amounts to seeing each measurement in the data twice. We found that increasing the learning rate had no visible benefits and hence did not modify it.

Our Meta-method uses the same base architecture as Overfit and [Sztrajman et al. 2021], a two-layer MLP with 21 neurons per hidden layer. We observed that incorporating second-order gradients into the optimization leads to more consistent results across all tasks and therefore use MAML with k=10 inner-loop steps, which is made possible by the lightweight architecture (675 parameters in total). While using a meta-batchsize improved generalization for the previous task, we found that averaging the meta-gradients over batches here leads to a decrease in result quality and hence use a meta-batchsize of one. We use the classic 80%-20% train-test split for training, both for the MERL materials and the angular measurements within a MERL material, and show results on unseen test BRDFs in Fig. B2.

B.3 svBRDF Synthesis

We again use an encoder-decoder approach to solve this problem, similar to the one motivated by Henzler et al. [2021]. Their method uses an encoder-decoder architecture, where the encoder

Table A1. Algorithm setup and hyperparameters for our experiments and the approaches we compare against.

	RGB Textures	BRDF Encoding	svBRDF Synthesis
Publication	[Henzler et al. 2021]	[Sztrajman et al. 2021]	[Henzler et al. 2021]
Type	CNN	MLP	CNN
Rendering	_	Mitsuba [Jakob 2010]	Cook-Torrance
Input	RGB Image	MERL	Flash Image
Data	500 textures	[Matusik 2003]	[Henzler et al. 2021]
Meta Algorithm	FOMAML	MAML	FOMAML
Gradient Order	First	Higher	First
Cosine Annealing	Yes	No	Yes
Meta-SGD	Yes	Yes	Yes
Meta-SGD Init.	1×10^{-3}	1×10^{-3}	1×10^{-3}
Meta-Optimizer	Adam	Adam	Adam
Meta-Optim. LR	1×10^{-4}	1×10^{-4}	1×10^{-4}
Meta-Optim.			
Weight Decay	_	1×10^{-6}	_
Inner-Loop Steps	10	10	20
Meta-Batchsize	5	1	3
Meta Training Time	~ 2 days	~ 3 days	~ 4 days
Meta Training Epochs	100,000	7.6×10^{6}	80,000
Time Meta-FW Pass	0.0220	0.00117	0.0309
Time Meta-Grad.Step	0.06185	0.00309	0.0742s
Time Meta-Inference	0.6185	0.0309	1.484s
Iterations Overfit	1,000	83,000	5,000
Iterations Finetune	100	1,000	1,000
Batchsize	4	512	4
Dimension Latent Space	64	10	64
Optimizer	Adam	Adam	Adam
Learning Rate	1×10^{-4}	5×10^{-4}	1×10^{-4}
LR Multiplier Finetune	10	1	10
Weight Decay	1×10^{-5}	_	1×10^{-5}
Training Loss	L1 VGG	Log. MAE	[Henzler et al. 2021]

Table B2. Different learning-rate and optimizer comparisons for the baseline methods we compare against. We choose the best-performing optmizer, respectively.

	0.1	0.01	0.001	1×10^{-4}	1×10^{-5}
Finetune, Adam	_	0.316	0.274	0.279	0379
Overfit, Adam	_	_	0.254	0.242	0.599
Finetune, SGD	0.713	0.397	0.360	0.486	_
Overfit, SGD	0.351	0.333	0.515	_	_

first projects a flash-illuminated image of a material into a latent space. The latent code is then used to condition the decoder, which is additionally provided with noise (for details, we refer to the publication) to then infer the svBRDF parameters. More specifically, the decoder outputs parameter maps of the Cook-Torrance [1982] reflectance model, i.e., diffuse and specular albedo, roughness and height, which is differentiated to a normal map. The generated

svBRDF maps are then rendered by a differentiable renderer, assuming collocated camera and light, flat geometry and stationarity, as elaborated on by Aittala et al. [2016].

We implement method <code>General</code> with the public code provided by Henzler et al. [2021], without fine-tuning, and train until convergence. For <code>Finetune</code>, we follow the method proposed in [Henzler et al. 2021] and fine-tune the learned general decoder for 1000 epochs, with the learning rate increased by a factor of 10. For <code>Overfit</code>, we train the decoder of <code>General</code> only, as there is no need to span a latent space when overfitting only a single exemplar. We additionally let the model learn the rotation parameters of the flash highlight, which, surprisingly, does not always put the flash in the center. We attribute this to the fact that minimizing the error between gram matrices, which is one of the main parts of the training loss, matches exemplar statistics globally and discards information about relative spatial layout. Note that the ratio of fine-tuning to over-fitting is 20%, which is remarkable.

Due to GPU memory constraints, our Meta-method for this application uses FOMAML, with k=20 gradient steps and a meta-batchsize of 3. We also experimented with lower amounts of inner-loop steps, but the results were not convincing. We attribute this to the ambiguity and under-constrained nature of the problem of estimating svBRDFs from a single image: While it may be relatively simple for a model to quickly learn RGB colors or statistics alone, inversely solving the rendering operation for the svBRDF-maps that created said colors or statistics is a much harder task. We note that it is not uncommon to use a large number of inner-loop steps when meta-learning on ambiguous problems: Tancik et al. [2021] use 64 steps on a Reptile-model to meta-learn an MLP that approximates neural radiance fields.

We show inference results for unseen test svBRDFs in Fig. B3. We further show the parameter maps produced by our method, to prove that they are free of baked shading. This can also be proven by construction, as only non-stationary parameter maps can bake non-stationary shading into albedo. Stationary maps (like the ones we use) can, by construction, not bake-in non-stationary shading, as explained by [Aittala et al. 2016] and [Henzler et al. 2021]. Proving this, we have re-lit our results following the protocol in Henzler2021 and achieved relit-errors (VGG Gram L1, less is better) of 0.25 / 0.10 / 0.12 / 0.16 for GENERAL/OVERFIT/FINETUNE/META, respectively.

· ·

REFERENCES

- Jonas Adler and Ozan Öktem. 2018. Learned primal-dual reconstruction. *IEEE transactions on medical imaging* 37, 6 (2018).
- Miika Aittala, Timo Aila, and Jaakko Lehtinen. 2016. Reflectance modeling by neural texture synthesis. ACM Trans. Graph. (Proc. SIGGRAPH) 35, 4 (2016).
- Alexander William Bergman, Petr Kellnhofer, and Gordon Wetzstein. 2021. Fast training of neural lumigraph representations using meta learning. In NIPS.
- Sai Bi, Stephen Lombardi, Shunsuke Saito, Tomas Simon, Shih-En Wei, Kevyn Mcphail, Ravi Ramamoorthi, Yaser Sheikh, and Jason Saragih. 2021. Deep relightable appearance models for animatable faces. ACM Transactions on Graphics (TOG) 40, 4 (2021),
- Robert L Cook and Kenneth E. Torrance. 1982. A reflectance model for computer graphics. ACM Trans. Graph. 1, 1 (1982).
- Kristin J Dana and Jing Wang. 2004. Device for convenient measurement of spatially varying bidirectional reflectance. JOSA A 21, 1 (2004).
- Tristan Deleu, Tobias Würfl, Mandana Samiei, Joseph Paul Cohen, and Yoshua Bengio. 2019. Torchmeta: A Meta-Learning library for PyTorch. arXiv:1909.06576
- Valentin Deschaintre, Miika Aittala, Fredo Durand, George Drettakis, and Adrien Bousseau. 2018. Single-image svbrdf capture with a rendering-aware deep network. ACM Trans. Graph. (Proc. SIGGRAPH) 37, 4 (2018).
- Valentin Deschaintre, George Drettakis, and Adrien Bousseau. 2020. Guided Fine-Tuning for Large-Scale Material Transfer. In Comp. Graph. Forum, Vol. 39.
- Julie Dorsey, Holly Rushmeier, and François Sillion. 2010. Digital modeling of material appearance. Elsevier.
- Ron O Dror, Edward H Adelson, and Alan S Willsky. 2001. Recognition of surface reflectance properties from a single image under unknown real-world illumination. CVPR (2001).
- Alexei A Efros and Thomas K Leung. 1999. Texture synthesis by non-parametric sampling. In ICCV.
- Chelsea Finn, Pieter Abbeel, and Sergey Levine. 2017. Model-agnostic meta-learning for fast adaptation of deep networks. In ICML.
- John Flynn, Michael Broxton, Paul Debevec, Matthew DuVall, Graham Fyffe, Ryan Overbeck, Noah Snavely, and Richard Tucker. 2019. Deepview: View synthesis with learned gradient descent. In CVPR.
- Duan Gao, Xiao Li, Yue Dong, Pieter Peers, Kun Xu, and Xin Tong. 2019. Deep inverse rendering for high-resolution SVBRDF estimation from an arbitrary number of images. ACM Trans. Graph. 38, 4 (2019), 134–1.
- Leon A Gatys, Alexander S Ecker, and Matthias Bethge. 2015. A neural algorithm of artistic style. arXiv:1508.06576 (2015).

- Stamatios Georgoulis, Konstantinos Rematas, Tobias Ritschel, Efstratios Gavves, Mario Fritz, Luc Van Gool, and Tinne Tuytelaars. 2017. Reflectance and natural illumination from single-material specular objects using deep learning. *IEEE PAMI* 40, 8 (2017).
- Ian J Goodfellow, Jonathon Shlens, and Christian Szegedy. 2014. Explaining and harnessing adversarial examples. arXiv preprint arXiv:1412.6572 (2014).
- Darya Guarnera, Giuseppe Claudio Guarnera, Abhijeet Ghosh, Cornelia Denk, and Mashhuda Glencross. 2016. BRDF representation and acquisition. 35, 2 (2016).
- Yu Guo, Cameron Smith, Miloš Hašan, Kalyan Sunkavalli, and Shuang Zhao. 2020. MaterialGAN: reflectance capture using a generative svBRDF model. arXiv:2010.00114 (2020).
- David Ha, Andrew Dai, and Quoc V Le. 2016. Hypernetworks. *arXiv:1609.09106* (2016). Kaiming He, Xiangyu Zhang, Shaoqing Ren, and Jian Sun. 2016. Deep residual learning for image recognition. In *CVPR*.
- Philipp Henzler, Valentin Deschaintre, Niloy J Mitra, and Tobias Ritschel. 2021. Generative Modelling of BRDF Textures from Flash Images. ACM Trans Graph (Proc SIGGRAPH Asia) 40, 5 (2021).
- Philipp Henzler, Niloy J Mitra, and Tobias Ritschel. 2020. Learning a neural 3d texture space from 2d exemplars. In CVPR.
- Bingyang Hu, Jie Guo, Yanjun Chen, Mengtian Li, and Yanwen Guo. 2020. DeepBRDF:

 A Deep Representation for Manipulating Measured BRDF. In *Comp. Graph. Forum*,
 Vol. 39
- Xuecai Hu, Haoyuan Mu, Xiangyu Zhang, Zilei Wang, Tieniu Tan, and Jian Sun. 2019. Meta-SR: A magnification-arbitrary network for super-resolution. In CVPR.
- Xun Huang and Serge Belongie. 2017. Arbitrary style transfer in real-time with adaptive instance normalization. In *ICCV*.
- Wenzel Jakob. 2010. Mitsuba renderer. http://www.mitsuba-renderer.org.
- Bela Julesz. 1975. Experiments in the visual perception of texture. Scientific American 232, 4 (1975).
- Alexandr Kuznetsov, Milos Hasan, Zexiang Xu, Ling-Qi Yan, Bruce Walter, Nima Khademi Kalantari, Steve Marschner, and Ravi Ramamoorthi. 2019. Learning generative models for rendering specular microgeometry. ACM Trans. Graph. 38, 6 (2019)
- Alexandr Kuznetsov, Krishna Mullia, Zexiang Xu, Miloš Hašan, and Ravi Ramamoorthi. 2021. NeuMIP: multi-resolution neural materials. *ACM Trans. Graph. (Proc. SIGGRAPH)* 40. 4 (2021).
- Hendrik PA Lensch, Jan Kautz, Michael Goesele, Wolfgang Heidrich, and Hans-Peter Seidel. 2003. Image-based reconstruction of spatial appearance and geometric detail. ACM Trans. Graph. 22, 2 (2003).
- Zhenguo Li, Fengwei Zhou, Fei Chen, and Hang Li. 2017. Meta-sgd: Learning to learn quickly for few-shot learning. arXiv:1707.09835 (2017).
- Guilin Liu, Duygu Ceylan, Ersin Yumer, Jimei Yang, and Jyh-Ming Lien. 2017. Material editing using a physically based rendering network. In CVPR.
- Stephen Lombardi and Ko Nishino. 2012. Reflectance and natural illumination from a single image. In ECCV. Springer.
- Wojciech Matusik. 2003. A data-driven reflectance model. Ph.D. Dissertation. Massachusetts Institute of Technology.
- Maxim Maximov, Laura Leal-Taixé, Mario Fritz, and Tobias Ritschel. 2019. Deep appearance maps. In ICCV.
- Ben Mildenhall, Pratul P Srinivasan, Matthew Tancik, Jonathan T Barron, Ravi Ramamoorthi, and Ren Ng. 2020. Nerf: Representing scenes as neural radiance fields for view synthesis. In ECCV.
- Giljoo Nam, Joo Ho Lee, Diego Gutierrez, and Min H Kim. 2018. Practical svbrdf acquisition of 3d objects with unstructured flash photography. ACM Trans. Graph. (TOG) 37, 6 (2018).
- Addy Ngan, Frédo Durand, and Wojciech Matusik. 2005. Experimental Analysis of BRDF Models. *Rendering Techniques* (2005).
- Alex Nichol, Joshua Achiam, and John Schulman. 2018. On first-order meta-learning algorithms. arXiv:1803.02999 (2018).
- Jannik Boll Nielsen, Henrik Wann Jensen, and Ravi Ramamoorthi. 2015. On optimal, minimal BRDF sampling for reflectance acquisition. ACM Trans. Graph. (Proc. SIGGRAPH Asia) 34, 6 (2015).
- Jeong Joon Park, Peter Florence, Julian Straub, Richard Newcombe, and Steven Lovegrove. 2019. DeepSDF: Learning continuous signed distance functions for shape representation. In CVPR.
- Adam Paszke, Sam Gross, Francisco Massa, Adam Lerer, James Bradbury, Gregory Chanan, Trevor Killeen, Zeming Lin, Natalia Gimelshein, Luca Antiga, Alban Desmaison, Andreas Kopf, Edward Yang, Zachary DeVito, Martin Raison, Alykhan Tejani, Sasank Chilamkurthy, Benoit Steiner, Lu Fang, Junjie Bai, and Soumith Chintala. 2019. PyTorch: An Imperative Style, High-Performance Deep Learning Library. In NIPS.
- Lara Raad, Axel Davy, Agnès Desolneux, and Jean-Michel Morel. 2018. A survey of exemplar-based texture synthesis. Annals of Mathematical Sciences and Applications 3, 1 (2018).
- Gilles Rainer, Abhijeet Ghosh, Wenzel Jakob, and Tim Weyrich. 2020. Unified neural encoding of BTFs. In Comp. Graph. Forum, Vol. 39.

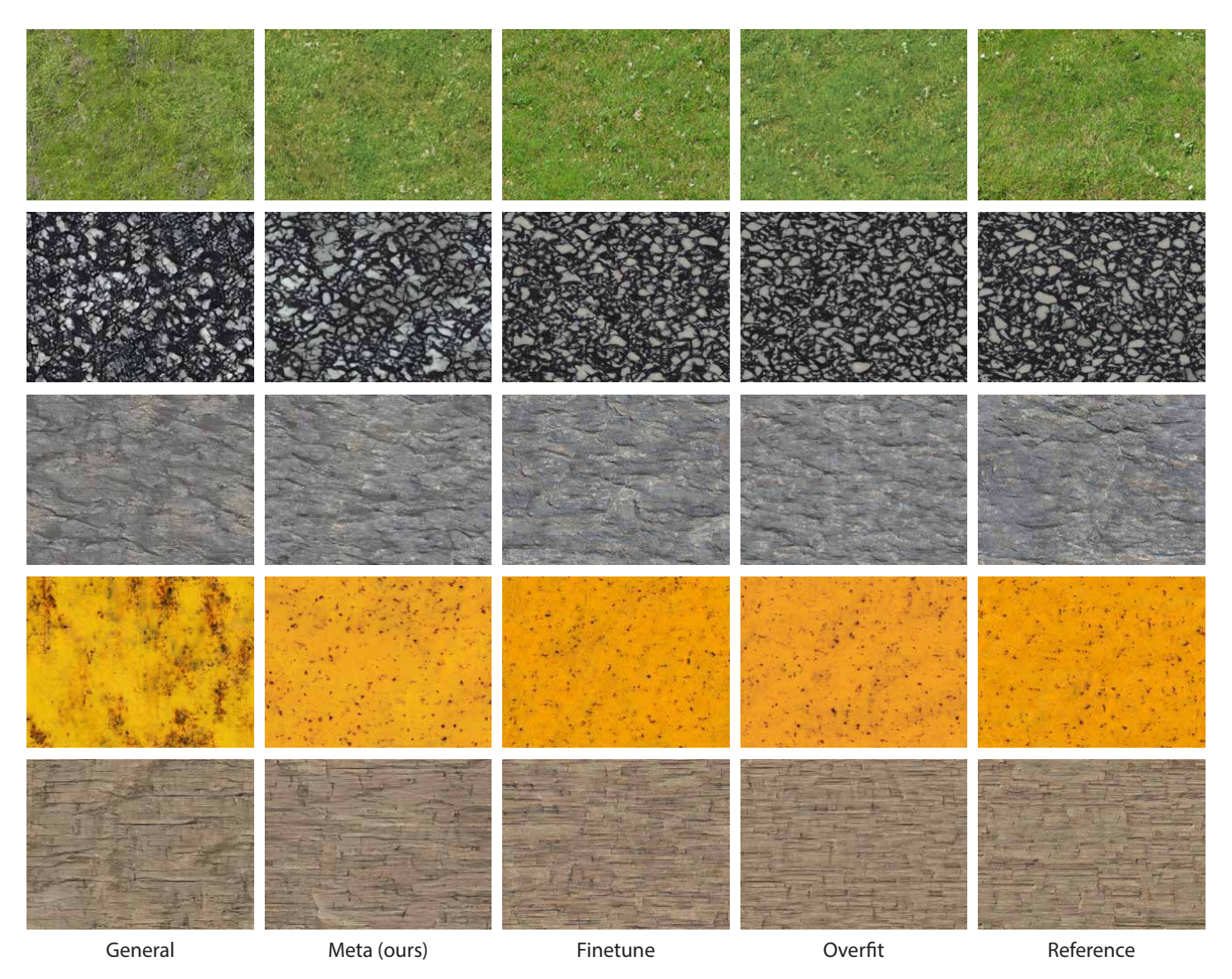


Fig. B1. Inference results for the test textures from the classes Grass, Marble, Rock, Rust, Wood (top to bottom row)

Gilles Rainer, Wenzel Jakob, Abhijeet Ghosh, and Tim Weyrich. 2019. Neural BTF compression and interpolation. In Comp. Graph. Forum, Vol. 38.

Olaf Ronneberger, Philipp Fischer, and Thomas Brox. 2015. U-net: Convolutional networks for biomedical image segmentation. In MICCAI.

Szymon M Rusinkiewicz. 1998. A new change of variables for efficient BRDF representation. In EGWR.

Vincent Sitzmann, Eric R Chan, Richard Tucker, Noah Snavely, and Gordon Wetzstein. 2020. MetaSDF: Meta-learning signed distance functions. arXiv:2006.09662 (2020).

Vincent Sitzmann, Michael Zollhöfer, and Gordon Wetzstein. 2019. Scene representation networks: Continuous 3d-structure-aware neural scene representations. arXiv:1906.01618 (2019).

Alejandro Sztrajman, Gilles Rainer, Tobias Ritschel, and Tim Weyrich. 2021. Neural BRDF Representation and Importance Sampling. In *Comp. Graph. Forum*, Vol. 40. Shufeng Tan and Michael L Mayrovouniotis. 1995. Reducing data dimensionality through optimizing neural network inputs. *AIChE Journal* 41, 6 (1995).

Matthew Tancik, Ben Mildenhall, Terrance Wang, Divi Schmidt, Pratul P Srinivasan, Jonathan T Barron, and Ren Ng. 2021. Learned initializations for optimizing coordinate-based neural representations. In CVPR.

Ayush Tewari, Ohad Fried, Justus Thies, Vincent Sitzmann, Stephen Lombardi, Kalyan Sunkavalli, Ricardo Martin-Brualla, Tomas Simon, Jason Saragih, Matthias Nießner, et al. 2020. State of the art on neural rendering. In *Comp. Graph. Forum*, Vol. 39.

 $\label{thm:point} Dmitry Ulyanov, Vadim Lebedev, Andrea Vedaldi, and Victor S Lempitsky. 2016. Texture networks: Feed-forward synthesis of textures and stylized images.. In {\it ICML}.$

Shaofei Wang, Marko Mihajlovic, Qianli Ma, Andreas Geiger, and Siyu Tang. 2021. MetaAvatar: Learning Animatable Clothed Human Models from Few Depth Images. arXiv:2106.11944 (2021).

Xiuming Zhang, Pratul P Srinivasan, Boyang Deng, Paul Debevec, William T Freeman, and Jonathan T Barron. 2021. NeRFactor: Neural Factorization of Shape and Reflectance Under an Unknown Illumination. arXiv:2106.01970 (2021).



Fig. B2. Inference results for the test BRDFS violet-acrylic, two-layer-silver, beige-fabric (top to bottom row) from the MERL dataset



Fig. B3. Inference results for the test svBRDFs. We show the comparison between Meta and the other training procedures, and additionally display the svBRDF parameter maps produced by Meta in every other row. To stress that Meta does not bake shading into either of the maps, we further provide a re-lit rendering, illuminated with a top-light.